NEOPLASIA
www.neoplasia.com

Volume 13 Number 10 October 2011 pp. 931–946 **931**

Hepatic Carcinoma–Associated Fibroblasts Promote an Adaptative Response in Colorectal Cancer Cells That Inhibit Proliferation and Apoptosis: Nonresistant Cells Die by Nonapoptotic Cell Death[1]

Mireia Berdiel-Acer*,†, Monika E. Bohem*, Adriana López-Doriga‡, August Vidal§, Ramon Salazar¶, Maria Martínez-Iniesta*, Cristina Santos¶, Xavier Sanjuan§, Alberto Villanueva* and David G. Molleví*

*Laboratory of Translational Research, Institut Català d'Oncologia-IDIBELL, Hospitalet de Llobregat, Barcelona, Spain; †Department of Medicine, Autonomous University of Barcelona, Bellaterra, Barcelona, Spain; ‡Bioinformatics Unit, Institut Català d'Oncologia-IDIBELL, Hospitalet de Llobregat, Barcelona, Spain; §Pathology Department, Hospital Universitari de Bellvitge-IDIBELL, Hospitalet de Llobregat, Barcelona, Spain; ¶Medical Oncology Department, Institut Català d'Oncologia-IDIBELL, Hospitalet de Llobregat, Barcelona, Spain

Abstract

Carcinoma-associated fibroblasts (CAFs) are important contributors of microenvironment in determining the tumor's fate. This study aimed to compare the influence of liver microenvironment and primary tumor microenvironment on the behavior of colorectal carcinoma. Conditioned medium (CM) from normal colonic fibroblasts (NCFs), CAFs from primary tumor (CAF-PT) or liver metastasis (CAF-LM) were obtained. We performed functional assays to test the influence of each CM on colorectal cell lines. Microarray and gene set enrichment analysis (GSEA) were performed in DLD1 cells cultured in matched CM. In DLD1 cells, CAF-LM CM compared with CAF-PT CM and NCF led to a more aggressive phenotype, induced the features of an epithelial-to-mesenchymal transition more efficiently, and stimulated migration and invasion to a greater extent. Sustained stimulation with CAF-LM CM evoked a transient G_2/M cell cycle arrest accompanied by a reduction of apoptosis, inhibition of proliferation, and decreased viability of SW1116, SW620, SW480, DLD1, HT-29, and Caco-2 cells and provoked nonapoptotic cell death in those cells carrying *KRAS* mutations. Cells resistant to CAF-LM CM completely changed their morphology in an extracellular signal–regulated protein kinase–dependent process and depicted an increased stemness capacity alongside the Wnt pathway stimulation. The transcriptomic profile of DLD1 cells treated with CAF-LM CM was associated with Wnt and mitogen-activated protein kinase pathways activation in GSEA. Therefore, the liver microenvironment induces more efficiently the aggressiveness of colorectal cancer cells than other matched microenvironments do but secondarily evokes cell death. Resistant cells displayed higher stemness capacity.

Neoplasia (2011) 13, 931–946

Abbreviations: CAF-PT, carcinoma-associated fibroblasts from primary tumor; CAF-LM, carcinoma-associated fibroblasts from liver metastasis; NCF, normal colonic fibroblast; CM, conditioned medium; GSEA, gene set enrichment analysis

Address all correspondence to: David G. Molleví, PhD, Laboratori de Recerca Translacional, Institut Català d'Oncologia-IDIBELL, Hospital Duran i Reynals, 3a planta, Av Gran Via 199-203, 08907 L'Hospitalet de Llobregat, Barcelona, Spain. E-mail: dgmollevi@iconcologia.net

[1]This work was supported by a grant from the Spanish Ministry of Health (FIS PI07-0657). The authors declare that there are no conflicts of interests.
Received 17 May 2011; Revised 16 August 2011; Accepted 23 August 2011

DOI 10.1593/neo.11706

Introduction

Tissue stroma has a dual role in controlling normal and malignant development: it impedes neoplastic growth in normal tissues, whereas it potentiates invasion and tumor growth in cancer progression [1], being summarized this latter aspects in relevant reviews [2–4]. Therefore, cancer cannot be understood as a malignant cell-exclusive process anymore. Instead, cancer is viewed as a complex tissue where different cell types interact heterotypically, creating a particular microenvironment where cells embedded in the extracellular matrix coexist. The balance of those populations, plus the composition of this extracellular matrix, could determine the tumor's fate.

In desmoplastic tumors, the more representative cells are carcinoma-associated fibroblasts (CAFs). CAFs play an important role contributing to modulate the tumor's fate because these cells are able to establish paracrine communication with other cell types inside the cancerous ecosystem to enhance angiogenesis [5], epithelial-to-mesenchymal transition (EMT) induction [6], and invasiveness [7], as well as to influence the effect of antitumoral drugs on malignant cells [8]. However, different microenvironments (liver, colon, etc) may produce different stimuli on cancerous cells. To clarify such discrepancy, we studied the effect of three different, but paired, microenvironments where the colorectal tumoral cells coexists in their life span to get to know the different contributions of each microenvironment to the malignant capabilities of cancer cells.

Metastatic capabilities are widely considered as a consequence of the acquisition of novel genetic changes in epithelial cells. However, we describe the ability of the conditioned medium (CM) from CAFs derived from a liver metastasis (CAF-LM) to enhance the aggressiveness (migration and invasion) of colorectal cell lines more effectively than paired CM from normal colonic fibroblasts (NCFs) and CAFs from the primary tumor (CAF-PT). However, if CAF-LM CM is sustained, it decreases viability and induces colorectal cancer cell death. Colorectal cells resistant to such delayed stimuli expressed a specific transcriptomic profile associated with cytoskeleton remodeling and Wnt and mitogen-activated protein kinase (MAPK) pathways activation determined by gene set enrichment analysis (GSEA).

Materials and Methods

Fibroblast Cultures and Preparation of CM

We obtained fibroblast cultures from fresh surgical specimens resected from patients with colorectal carcinoma (NCF from the normal colonic mucosa at least 5 cm from the surgical margin and CAF-PT and CAF-LM from a synchronous metastasis in the case of the matched triplet) under the supervision of the ethics committee of the Hospital Universitari de Bellvitge. Fibroblasts and CAFs were cultured in Dulbecco modified Eagle medium (DMEM)/F12 +10% fetal bovine serum (FBS; Gibco, Grand Island, NY) with added penicillin/streptomycin. After four or five passages, cells in confluence were harvested, and cultures were used to make CM. They were then washed twice with phosphate-buffered saline (PBS) and cultured in DMEM/F12 free from FBS. After 48 hours of incubation, CM from the five plates were collected and mixed in one vial. CM were centrifuged for 5 minutes at 3000 rpm, filtered through 22-μm units, and stored at −80°C until use. Next, fibroblast/CAF cultures were washed twice with PBS and incubated for 48 hours in DMEM/F12 (containing 10% FBS). We used CM with 10% FBS for long-term assays and DMEM/F12 free from FBS for proteomics and extracellular signal–regulated protein kinase (ERK) stimulation.

Wound Healing Assay and Migration Assay

DLD1 cells were seeded in 6-cm-diameter plates and cultured until confluent. After 12 hours of culture in serum-free DMEM/F12, the plate was scratched with a yellow 200-μl pipette tip to create the wound. After several PBS washes to remove floating cells, pictures were taken at 1, 3, 5, 7, and 24 hours. Distances between cell margins were measured with Leica software (Wetzlar, Germany). We conducted the assay in duplicate, measuring the distances between the two fronts at three points and culturing cells with matched CM or with nonmatched CM (NCF, CAF-PT, and CAF-LM, $n = 3$ each).

For the transwell migration assay, we used 96-well high-throughput screening plates with Transwell chambers (Corning, Lowell, MA) containing polycarbonate membrane filters (pore size, 8 μm). DLD1 cells (5×10^4) were plated in the upper chamber and stimulated with DMEM/F12 or CM from different fibroblasts and CAFs. After 24 hours, cells that invaded the undersurface of the membrane were stained with crystal violet. The dye was eluted, and the absorbance measured at 590 nm.

Invasion Assay

Ninety-six–well HTS plates with Transwell chambers containing polycarbonate membrane filters (pore size, 8 μm) were coated with 0.2× basal membrane extract (BME; Trevigen, Gaithersburgh, MD) or 1× BME. A total of 5×10^4 DLD1 or SW480 cells were plated in the upper chamber and stimulated with DMEM/F12 or CM from different fibroblasts and CAFs. After 48 hours, cells that invaded the undersurface of the membrane were stained with Calcein AM (Trevigen) for 1 hour, and the resulting fluorescence intensity was measured in a fluorescence reader with filters set to 485 nm of excitation and 520 nm of emission. As a control, we used hepatocyte growth factor 40 ng/ml (R&D Systems, Minneapolis, MN).

Proliferation Assay

WST-1 cell proliferation assay was conducted following the manufacturer's instructions (PreMix WST-1 Proliferation Assay; Takara, Shiga, Japan). Briefly, 1×10^4 serum-starved cells (colorectal cell lines) were seeded in 96-well plates and cultured at different times in DMEM/F12 or the appropriate matched CM. We reproduced results in nonmatched CM. After the assay, the culture medium was then replaced by 10 μl of WST-1 reagent in 100 μl of serum-free DMEM/F12 and incubated for a further 2 hours. Absorbance was measured at 450 nm.

We also reproduced experiments in crystal violet staining.

Quantitative Real-time Reverse Transcription–Polymerase Chain Reaction Analysis

Total RNA was retrieved from all fibroblasts using TRIzol reagent method and column purification. Quantitative real-time reverse transcription–polymerase chain reaction analyses were performed using the LightCycler 2.0 Roche System and LightCycler FastStart DNA Master SyBR Green I kit (Roche, Mannheim, Germany). Slug, Snail, ZEB-1, N-cadherin, and E-cadherin primers will be provided on request. For normalization of expression levels, we analyzed the expression of glyceraldehyde-3-phosphate dehydrogenase. All of the experiments were performed in triplicate using two different retrotranscriptions.

Colony-Forming Assay

We plated 1000 cells in 6-cm-diameter culture dishes and incubated for 15 days in DMEM/F12 (control) or different CM. We evaluated the number of colonies after crystal violet staining.

Microarray and GSEA

Total messenger RNA (mRNA) from DLD1 cells cultured for 48 hours in DMEM/F12 or CM (five culture plates each condition) was mixed in four pooled mRNA samples and hybridized in GeneChip Human Genome U133 Plus 2.0 (Affymetrix, High Wycombe, United Kingdom). Details of isolating mRNA, labeling, and hybridizing are described elsewhere [9]. Raw microarray intensity data were corrected for background, normalized, and log-transformed using the robust multichip average algorithm [10]. Ratios of expression values between CM and DMEM/F12 were computed for all genes, establishing an ordered gene list according to expression changes.

Statistical analysis is based on a nonpaired Student's *t* test using SAM methodology [11]. Low variances tend to overestimate the level of significance, but this effect was avoided using the false discovery rate (FDR), selecting genes with FDR less than 0.01. Analysis was carried out using the R statistic software package.

Gene ontology was carried out using DAVID database.

Finally, GSEA algorithm was applied using Java implementation [12], with the gene lists ordered according to expression ratios. Statistical significance (FDR *q* and family-wise error rate *P*) of the enrichment score (ES) was calculated in the implementation using default values and by permuting the signatures' genes 1000 times for each analysis.

Cell Cycle Assessment and M-phase Ratio Evaluation

We followed classic procedures to evaluate propidium iodine (PI) staining DNA content. Briefly, we isolate single-cell suspensions. Cells were fixed with cold ethanol overnight at 4°C. We resuspended the pelleted cells in 800 μl of PBS containing 1% bovine serum albumin. Then we add 100 μl of 10× PI solution and 100 μl of RNase A (10 mg/ml) and incubate the mix at 37°C for 30 minutes. We analyzed the samples in a Gallios Flow Cytometer (Beckman Coulter, Krefeld, Germany).

To evaluate the proportion of cells that were in the M-phase of the cell cycle, we cultured nonsynchronized cells for 5 days in DMEM/F12 or CM. After 5 days, cells were fixed and stained with 4′,6-diamidino-2-phenylindole. Under the microscope, we counted the ratio of cells that displayed metaphasic plate or were entering in early cytokinesis.

In addition, using Western blot analysis, we checked the levels of P21 (no. OP67; Oncogene Research Products, La Jolla, CA), cyclin D1 (MS210-P; NeoMarkers, Fremont, CA), cyclin B1 (sc-595; Santa Cruz Biotechnology, Santa Cruz, CA), proliferating cell nuclear antigen (sc-25280; Santa Cruz Biotechnology), and polo-like kinase 1 (PLK1, 06-813; Millipore, Billerica, MA) to assess the control of the cell cycle arrest in G_2 and the entry in mitosis.

Wnt Pathway Activation

Using Western blot analysis, we assessed the effect of CM from CAF-LM on the overexpression of Wnt target cMyc in APC mutant (DLD1 cells) and APC wild-type (HCT-116) using the antibody anti–c-MYC (M4439 clone 9E10; Sigma, Tres Cantos, Madrid, Spain).

Furthermore, using double immunofluorescence, we evaluate the nuclear translocation of active β-catenin in DLD1 cells cultured for 5 days in DMEM or CM from NCF or CAFs (PT and LM) using anti–β-catenin (AB19022; Millipore) and anti–active β-catenin (anti-ABC, clone 8E7; Millipore).

Western Blot Analysis of ERK1/2 Phosphorylation

To evaluate the activation of the MAPK pathway in the presence of different CM, 5×10^5 DLD1 cells were grown in 6-cm-diameter dishes, serum-starved overnight, and treated with CM for 0, 10, 30, and 120 minutes. Twenty micrograms of protein from cell lysates was loaded into a 10% acrylamide gel and transferred to a polyvinylidene fluoride membrane. Membrane was blocked for 1 hour at room temperature in 10% nonfat milk and 0.1% Tween in PBS, washed, and incubated overnight at 4°C with anti–phospho p44/42 (Thr^{202}/Tyr^{204}) (Cell Signaling Technology) diluted 1:1000 in 1% nonfat milk.

Detection was performed using a horseradish peroxidase–conjugated secondary antimurine immunoglobulin G antibody and enhanced chemiluminescence (ECL Kit; Amersham, Arlington Heights, IL).

For the detection of total ERK levels, the membrane was washed with PBS, incubated with stripping buffer (30 minutes at 50°C), washed again, and blocked overnight at 4°C in 5% nonfat milk. Incubation was carried out for 1 hour at room temperature using the same anti–phospho p44/42 antibody. Detection was done as mentioned previously.

Determination of Caspase 3 Activity

Apoptosis was assessed using Ac-DEVD-AMC caspase 3 fluorogenic substrate (BD Pharmingen, San Agustin de Guadalix, Madrid, Spain) on adherent cells alone or adherent plus floating cells. Cell were lysed with lysis buffer containing 5 mM Tris-HCl, 20 mM EDTA, and 0.5% Triton X-100. For each reaction, we add 20 μM Ac-DEVD-AMC and cell lysate to 1 ml of protease assay buffer (1 M HEPES, 10% glycerol, 1 M dithiothreitol). We incubated the reaction mixtures for 2 hours at 37°C in the dark, and then we measured the AMC liberated from Ac-DEVD-AMC using a fluorimeter.

Statistical Methods

We first checked that data fitted a normal distribution with the Kolmogorov-Smirnov test. Statistical analysis was based on the nonparametric Mann-Whitney *U* test.

Results

CM from Hepatic CAF More Efficiently Enhances Migration of Colorectal Cells

First, we explored migration in a wound healing assay, stimulating cells with matched CM, and we observed that only cells cultured in CAF-LM CM migrated faster than that in control medium at all time points (Figure 1*A*, *upper panel* and microphotographs; Mann-Whitney *U* test for significance) and also faster than any other matched CM, completely closing the wound only when cultured with CAF-LM CM. We confirmed these results using different nonmatched CM (NCF, $n = 3$; CAF-PT, $n = 3$; CAF-LM, $n = 3$) both in a wound healing assay (Figure 1*A*, *lower panel*) and in a transwell assay (Figure 1*B*). SW480 depicted poor capabilities in migrating at least in the scratch assay.

To evaluate invasion, we checked the capabilities of DLD1 and SW480 to cross the transwell membrane in 48 hours in two conditions (we used HGF as a positive control):

First, in a mild matrix of 0.2× BME, CM from NCF, CAF-PT, and CAF-LM, which stimulated the invasiveness of DLD1 cells to the same extent (Mann-Whitney *U* test, $P = .05$ for all three CM in relation to DMEM/F12; Figure 1*C*, *left panel*, *red boxes*). No differences were observed between the three CM. For SW480 cells, transwell assay in 0.2× BME CAF-LM CM clearly conferred an invasive promoting effect, particularly in comparison with CAF-PT CM and HGF.

Second, in a dense 1× BME (Figure 1*C*, *blue boxes*), DLD1 cells clearly exhibited more capabilities than SW480 cells did, and there were no differences between CAF-PT and CAF-LM CM. In contrast,

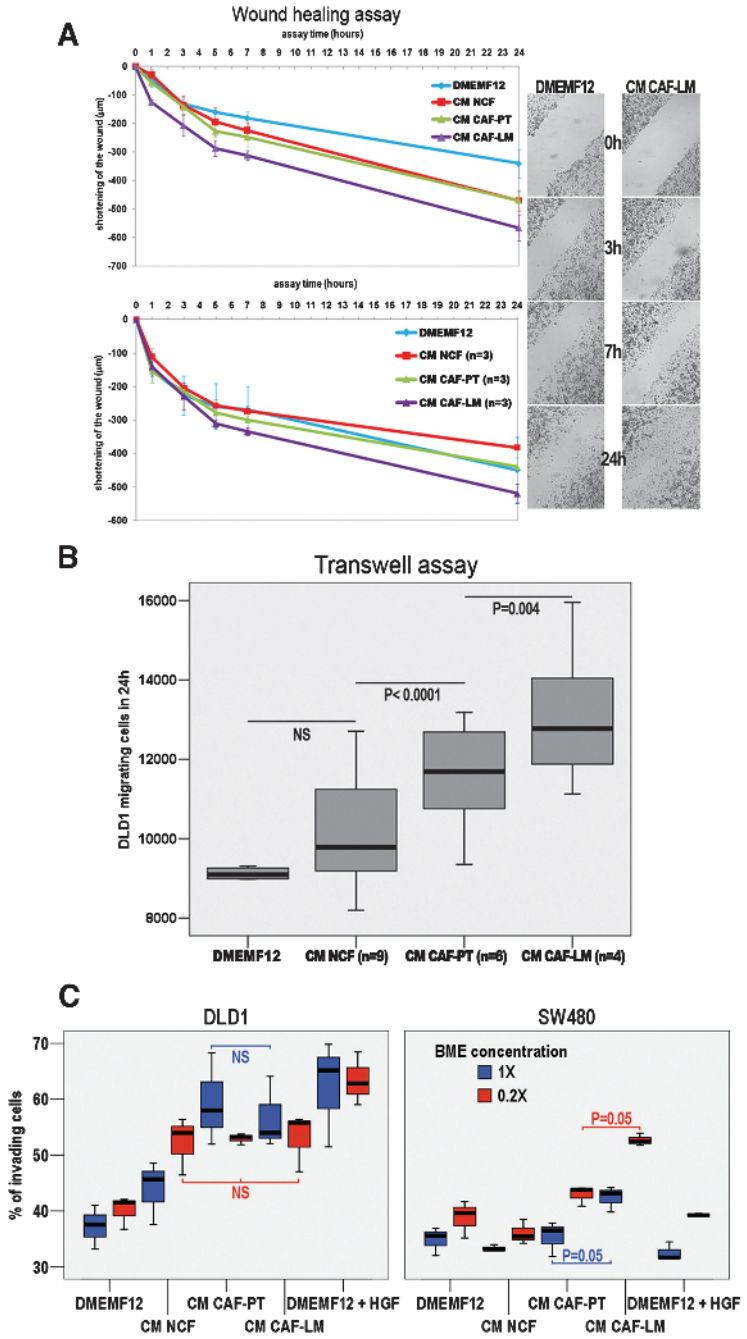

Figure 1. (A) Graphical representation of wound closure (residual wound distance) using CM from NCF, CAF-PT, and CAF-LM isolated from the same patient, showing the enhanced migrating ability of DLD1 cells cultured in CM from hepatic metastasis CAFs (upper panels and microphotograph). Results are mean values of two experiments consisting each of two plates for condition and three measures in the wound of each plate. Measures were taken at 1, 3, 5, 7, and 24 hours, respectively. CAF-LM treatment was statistically significant at all time points (Mann-Whitney U test, $P \leq .05$). Graphical representation of wound closure (residual wound distance) using nonmatched CM from NCF ($n = 3$), CAF-PT ($n = 3$), and CAF-LM ($n = 3$) (lower panels). Results are mean values of two experiments consisting each of two plates for condition and three measures in the wound of each plate. Measures were taken at 1, 3, 5, 7, and 24 hours. CAF-LM treatment was statistically significant after 24 hours of assay (Mann-Whitney U test, $P = .02$). (B) Box plots representing the migrating capabilities of DLD1 cells in different nonmatched CM from NCF, CAF-PT, and CAF-LM in a transwell assay. Values are median and upper and lower quartiles of three different experiments, eight replicates each (Mann-Whitney U test). (C) Invasion assay in transwell inserts with a lax 0.2× BME layer (red boxes) and dense 1 × BME layer (blue boxes). Box plot depicts percentage of cells that crossed the 8-μm pore size membrane (median of two experiments, eight replicates each). We used HGF (40 ng/ml) as a control to evaluate the invasive capabilities of each cell type because HGF is the most powerful stimulator of invasion for epithelial cells. Statistical significance was calculated first against control DMEM/F12 + 10% FBS or between CM (Mann-Whitney U test). In DLD1 cells, there were no statistical differences between CAF cell types: neither 0.2× BME nor 1× BME. On the contrary, CAF-LM CM conferred greater invasive capabilities than CAF-PT CM did for SW480 cells in both BME conditions (Mann-Whitney U test, $P = .05$).

SW480 cells in the CAF-LM CM definitely conferred greater invasion efficiency than matched CAF-PT CM did (Mann-Whitney *U* test, $P = .05$).

CAF-LM Induces Features of EMT in DLD1 Cells

Compared with control, the culture of DLD1 cells with CM from CAF-LM progressively induced the expression of transcription factors classically associated with EMT processes. As depicted in Figure 2*A*, the expression of ZEB-1, SNAI1, and SLUG increases with time, coinciding with an up-regulation of N-cadherin but not of E-cadherin. At the protein level, DLD1 cells cultured in DMEM/F12 show a junctional localization of E-cadherin but changed when culturing with CM from CAF-LM, displaying a cytoplasmic staining (Figure 2*B*, *upper panels*). The up-regulation of N-cadherin is clearly evident in Figure 2*B* (*lower panels*). Comparing paired CM from different locations, CAF-LM recapitulate more efficiently the features of the EMT, described as the expression of EMT-associated transcription factors (Figure 2*C*) and down-regulation of E-cadherin (Figure 2*D*).

CM from CAFs Stimulate Colony Formation

As shown in Figure 3*A*, the CM from all of the three types of myofibroblasts stimulates the formation of colonies in comparison

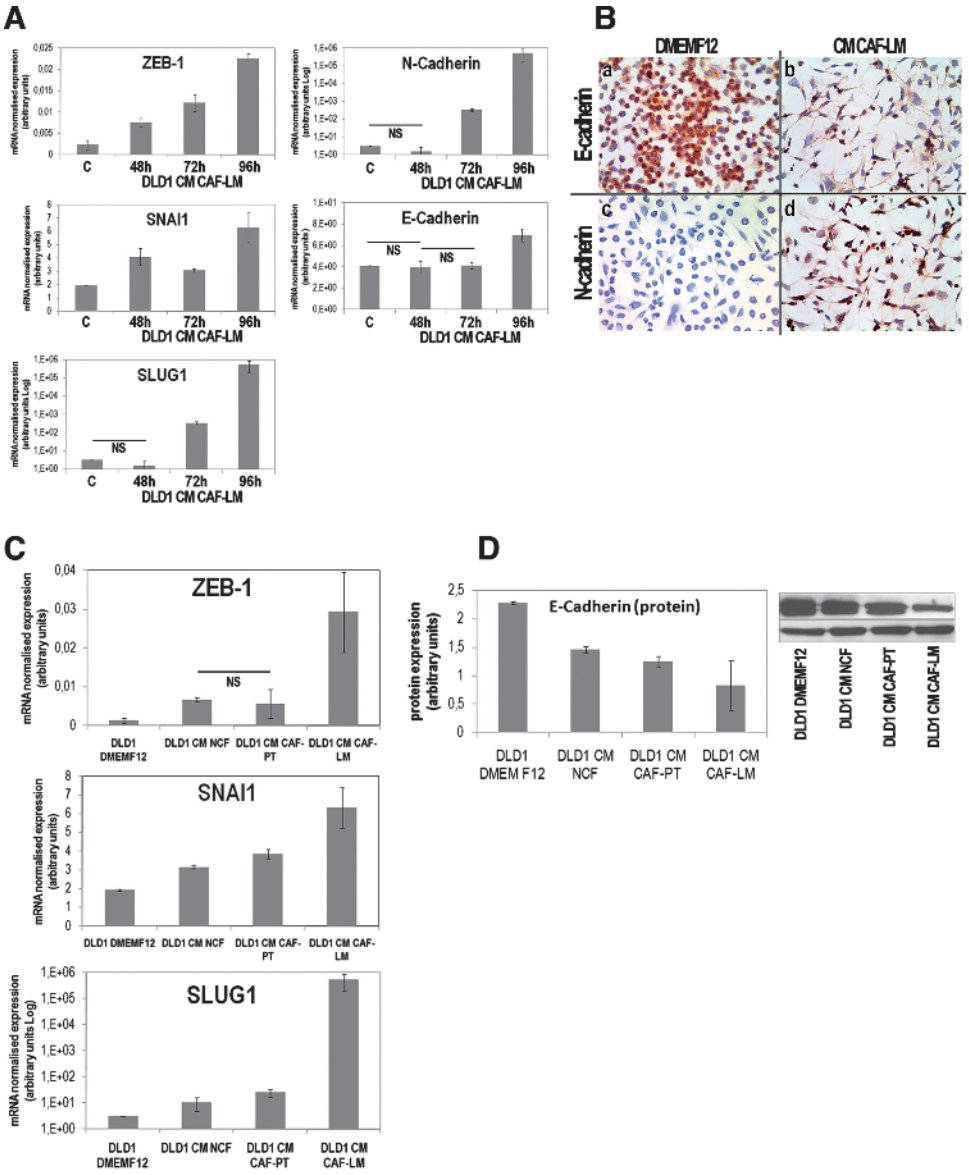

Figure 2. (A) Relative mRNA expression of EMT-associated genes (*ZEB1*, *SNAI1*, *SLUG1*, *E-cadherin*, and *N-cadherin*) in DLD1 colorectal cells at different assay times compared with control DMEM/F12. Values are mean ± SD from triplicates of two different experiments. All comparisons are significant (Mann-Whitney *U* test, $P < .05$), except for those marked as NS (nonsignificant). (B) Immunohistochemical staining of E-cadherin and N-cadherin (1:100 and 1:50, respectively; Becton Dickinson, San Agustin de Guadalix, Madrid, Spain) in DLD1 control cells and CAF-LM CM–treated DLD1 cells. (C) Relative mRNA expression of EMT-associated genes (*ZEB1*, *SNAI1*, *SLUG1*, *E-cadherin*, and *N-cadherin*) in DLD1 colorectal cells after 4 days in culture in different CM obtained from the same patient. Values are mean ± SD from triplicates of two different experiments. All comparisons are significant (Mann-Whitney *U* test, $P < .05$), except for those marked as NS (nonsignificant). (D) E-cadherin protein levels in DLD1 cells after 4 days in culture in different CM obtained from the same patient.

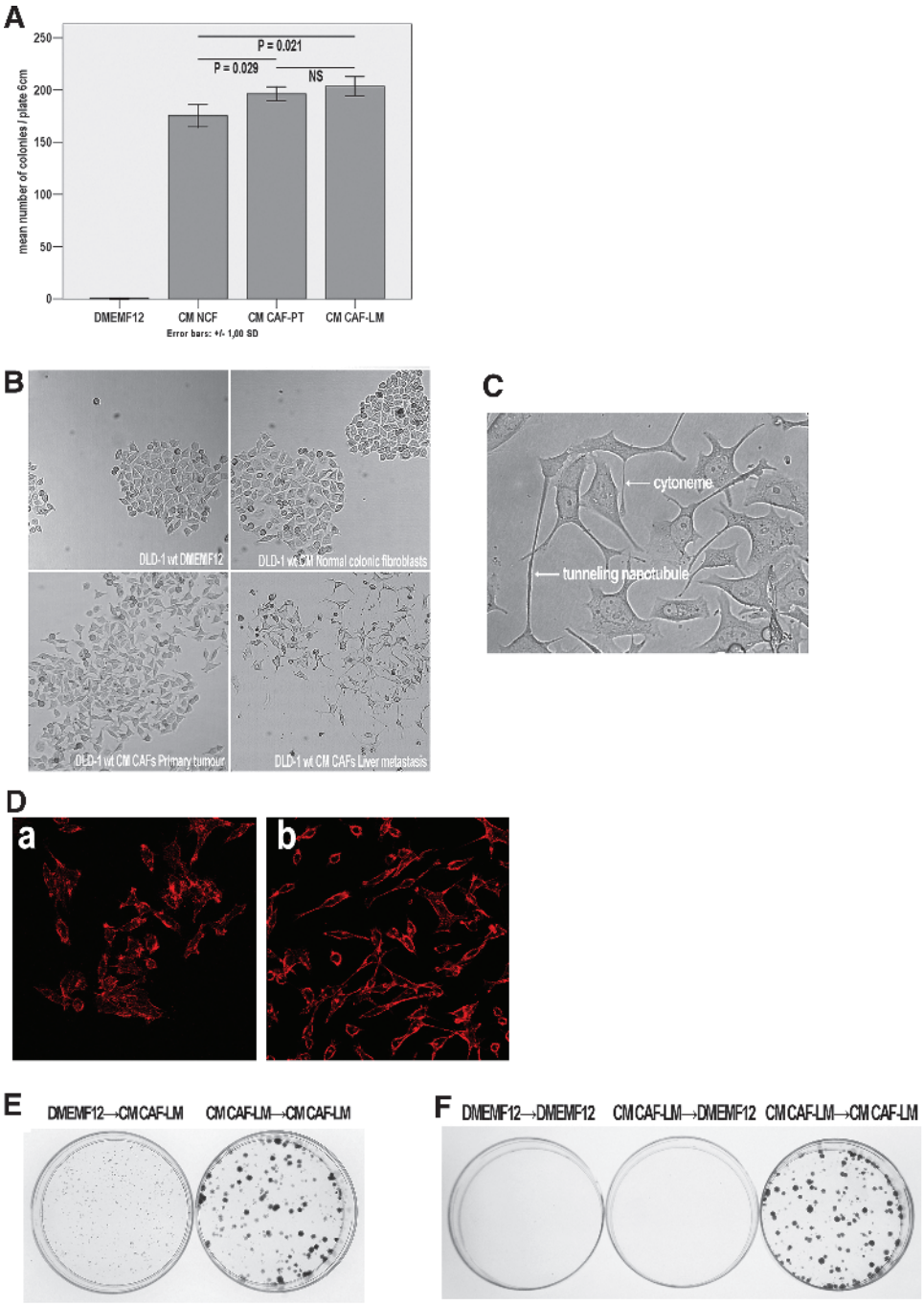

Figure 3. (A) Colony formation assay: We plated 1000 cells in 6-cm-diameter culture plates. After 15 days, no colonies were formed in DLD1 cells cultured in DMEM/F12 (control), and similar levels were counted for cells cultured in different CM, although there was a statistically significant difference between CM from NCFs and CAFs. Results are mean values of three experiments and three replicates each. (B) Morphology of DLD1 cell colonies cultured in DMEM/F12 + 10% FBS or different CM from NCF or CAFs in plastic culture plates. Specific phenotype was identified in DLD1 cells cultured with CM from CAFs from a liver metastasis, showing cytonemes and tunneling nanotubules. Such phenotype was evident after 48 hours of culture. (C) Detailed pictures (a and b) of the morphology of cells cultured in CAF-LM CM, showing long intercellular bridges. (D) F-actin staining (phalloidin red) in (a) DLD1 control and (b) DLD1 cultured in CAF-LM CM. (E) Comparison of the colonies size when culturing 1000 DLD1 cells in CAF-LM CM before a selective passage (left) or replating 1000 cells after a 5-day culture in CAF-LM CM (right). Replated survival cells depicted a more vigorous phenotype. (F) We cultured DLD1 cells in CAF-LM CM for 5 days, and then we replated 1000 cells again in CAF-LM CM or DMEM/F12. Only colonies were formed when cells were cultured in the CM.

to DMEM/F12 control. In addition, CM from CAFs produced a higher number of colonies than CM from NCF did. An interesting observation was the formation of cytonemes and tunneling nanotubules when culturing with CAF-LM CM (Figure 3, *B* and *C*), something that we had already suspected when we made the phalloidin staining (Figure 3*D*).

In addition, DLD1 cells were cultured for 5 days in CAF-LM CM and then replated to evaluate colony-forming capacity. Cells that were cultured again with CAF-LM CM produced bigger colonies in the same assay time than those that were not pretreated, although not increasing the number of colonies (Figure 3*E*). When replated cells were cultured with DMEM/F12, no colonies were obtained (Figure 3*F*).

CM from CAF-LM Decrease Both Viability and Apoptosis of Colorectal Cells and Induce Necrosis

Moreover, the addition of CM from fibroblasts of three different locations of the same patient differentially affects the viability of DLD1 and SW480 cells as measured with the WST-1 assay and crystal violet staining. As shown in Figure 4*A*, after 5 days of culture, both in DLD1 and in SW480 cells, CM from CAF-PT induced a significant increase in viability in relation to the control (DMEM/F12 + 10% FBS). On the contrary, CM from CAF-LM clearly displayed a significant decrease in cell viability, evidenced by a large number of floating cells. We validated these results using CM of different CAFs (CAF-PT, $n = 6$; CAF-LM, $n = 4$) and CRC *KRAS* mutant cell lines (DLD1, SW480, SW620, and SW1116), confirming that CAF-LM CM lead to a decrease of cell viability (Figure 4*B*) in comparison with CAF-PT CM. This was especially remarkable for cells derived from more advanced tumoral stages (DLD1 and SW620). To preclude a possible effect of nutrient depletion during the production process of CM, we repeated the experiments, using FBS-free CM, which was subsequently supplemented with FBS just at the moment of performing the experiment. We obtained the same results (Figure 4*C*). The behavior was the same for all cell lines.

We also checked cell CAF-LM CM–induced proliferation in *KRAS* wild-type cells (*BRAF* mutant HT-29 and *BRAF* wild-type Caco-2). We observed an increase in viability because we did not observe any floating cell after 5 days of culture, although the proliferation was also remarkably diminished (Figure 4*D*).

Therefore, our results clearly demonstrated that, compared with the control and CAF-PT CM, paired and nonpaired CM from CAF-LM were inhibiting proliferation on colorectal cell lines and decreasing viability in those carrying *KRAS* mutations.

To determine the durability of the CAF-LM–mediated inhibition of proliferation, tumor cells were cultured with CAF-LM CM for 5 days and then cells were harvested and replated for 48, 72, or 144 hours in normal culture medium (control) or CAF-LM CM to assess the recovering capacity from the inhibitory effect. After 48 hours, the pretreated cells displayed the same proliferative capacity than the control, but after 72 and 144 hours, the viability decreased by approximately 15% and 32%, respectively. These cells restored their normal cell morphology. Replated cells treated again with CAF-LM CM displayed poor proliferative capabilities, reaching a 75% reduction after 144 hours (Figure 4*E*). The same behavior was observed for HT-29 cells. Depending on the cells' plating density, the change of culture medium from CAF-LM CM to DMEM/F12 seems to favor the restoration of proliferative capabilities but diminish the stemness capacity, as depicted in Figure 4*F*.

Products Secreted by CAF Reduce the Apoptosis of Tumor Cells

Cells cultured in CAF-LM CM were arrested in G_2/M. Our results suggest that some products secreted by CAF-LM induced the death of tumor cells. According to this, we first checked the effect of CM on tumor cell apoptosis. When DLD1 cells were cultured with either CAF-PT CM or CAF-LM CM, the levels of caspase 3 activity were considerably lower than in those cultured with DMEM/F12 (control) or NCF CM (Figure 5*A*). Cells that remained attached to the culture plate displayed similar levels of caspase activity. Thus, caspase activity was evidenced basically on the floating cells fraction, showing that the large number of floating cells, while cultured with CAF-LM CM, does not correspond to apoptosis. Moreover, the formation of cytonemes was not reversed by the addition of caspase inhibitors.

Senescence was also excluded as the cause of the observed phenotype because β-galactosidase staining was negative and cells stained well with Calcein AM.

Furthermore, by assessing the DNA content by means of flow cytometric PI staining, we observed that cells cultured in NCF CM and CAF-TP CM seemed to be arrested in G_0/G_1, whereas cells cultured in CAF-LM CM were arrested in G_2/M (Table 1). To corroborate this observation and to provide a more accurate information, we cultured cells on glass cover slides for 5 days in DMEM/F12 (control) or different CM. Then the cells were fixed, and the nuclei were stained with DAPI. As depicted in Figure 5*B*, we observed a high proportion of cells in mitosis in cells treated with DMEM/F12, NCF CM, or CAF-PT CM, but almost no cells were starting mitosis after 5 days in CM from CAF-LM. In addition, there were a high number of cells that displayed stronger DAPI intensity, indicating that they contain a double charge of genetic material but without reaching or completing mitosis.

This led us to check for proteins that are involved in the control of cell cycle, especially in key events in the G_2-to-M transition. We found that all CM lead to a strong inhibition of cyclin B1, especially remarkable with CAF-LM CM. The expression of cyclin D1, which is expressed in early G_1, shows that, after 5 days of exposure to CAF-LM CM, there were fewer cells that were entering G_1. PLK1 also shows that mitosis is diminished in cells cultured with CAF-LM CM. Some of these proteins are under control of P21, which is overexpressed in cells cultured in CM from CAFs (Figure 5*C*).

CM from CAF-LM Differentially Induces a Sustained Activation of ERK in DLD1 Cells

Addition of different CM (FBS-free) from fibroblasts (both CAF and NCF) to DLD1 cells induced an increase in ERK1, but especially in ERK2 phosphorylation, compared with serum-free medium control, which did not induce phosphorylation. In each of the different CM, the levels of ERK phosphorylation were increased after 10 minutes of stimulation, but they were still sustained for 2 hours with CAF-LM CM, as opposed to all other CM where a decrease in phosphorylation was observed (Figure 6*A*).

Moreover, the addition of a MEK inhibitor to the CAF-LM CM inhibited the development of cytonemes, tunneling nanotubules, and microvesicles, and the cells kept their normal appearance (Figure 6*B*).

Adding MEK inhibitor U0126 (20, 40, and 80 μM) to the CAF-LM CM profoundly affected proliferation, whereas ERK inhibitor FR180204 (50, 100, and 200 μM) had only little or no effect on proliferation (data not shown).

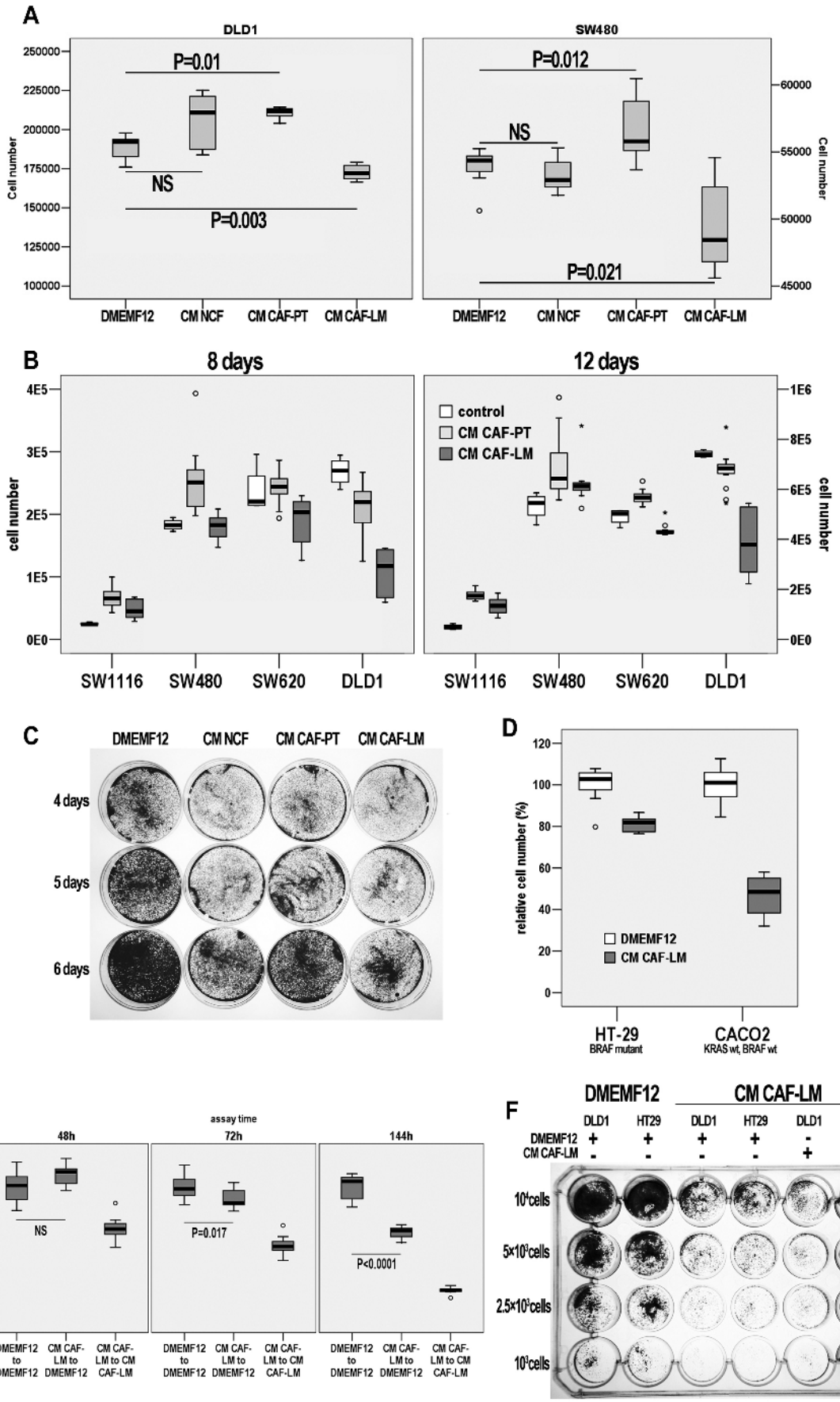
A
DLD1
SW480
P=0.01
NS
P=0.003
P=0.012
NS
P=0.021
Cell number
DMEMF12
CM NCF
CM CAF-PT
CM CAF-LM
B
8 days
12 days
control
CM CAF-PT
CM CAF-LM
cell number
SW1116
SW480
SW620
DLD1
C
DMEMF12
CM NCF
CM CAF-PT
CM CAF-LM
4 days
5 days
6 days
D
relative cell number (%)
DMEMF12
CM CAF-LM
HT-29
BRAF mutant
CACO2
KRAS wt, BRAF wt
E
assay time
48h
72h
144h
Relative cell count
NS
P=0.017
P<0.0001
DMEMF12 to DMEMF12
CM CAF-LM to DMEMF12
CM CAF-LM to CM CAF-LM
F
DMEMF12
CM CAF-LM
DLD1
HT29
DMEMF12 + + + + - -
CM CAF-LM - - - - + +
10⁴cells
5x10³cells
2.5x10³cells
10³cells

Products Secreted by Hepatic CAFs Modify the Expression Profile in Colorectal Cell Lines

DLD1 cells cultured in CAF-LM CM clearly exhibit a completely different genetic profile compared with DLD1 cells in standard culture conditions or other CM.

Of the 54,000 probes we screened, we identified a total of 33 that were exclusively upregulated (fold change >2) in CAF-LM CM–cultured cells (Table 2). Among them were genes related to cytoskeleton reorganization (as expected given the formation of cytonemes) and invasiveness, namely, *ARF6*, *ACTR2*, *RHOB*, and *MALAT1*, and relevant genes in colorectal tumorigenesis, namely, *CDH1*, *CTNNB1*, *DDX17*, and *MAP3K1*, which are important regulators of Ras-ERK and Wnt pathways. The most overexpressed gene was *PRSS1*, which encodes trypsinogen, a serine protease involved in pancreatitis. Among the 53 underexpressed probes, there are several that correlate with proliferation (*Ki67*, *cyclin E2*, *CDCA3*, *CDC45L*), mitosis, cytokinesis, and cell cycle progression (*ECT2*, *KIF14*, *KIF15*, *PLK1*, *survivin*, and *CENPA*), which is in line with our previous experimental observation of reduced proliferation in CAF-LM CM–treated cell lines. Gene ontology analysis correlated bioinformatic data with functional assays and revealed that significantly overexpressed genes were involved in the processes of response to stimulus and wound healing (Table 3). Downregulated genes corresponded basically to cell cycle control genes.

GSEA Associated Deregulated Probes in Cells Cultured in CM from CAF-LM with Mechanisms Involved in Metastatic Processes

GSEA is a computational method that determines whether an *a priori*–defined set of genes shows statistically significant, concordant differences between two biologic states and is a powerful tool to identify significant and coordinated changes in gene expression data. According to this, we searched for signaling pathways associated with the most representative genes found to be deregulated in our previous experiments. The most significant ones (FWER $P < .02$) are summarized in Table 4. We could collapse these pathways basically in four categories: cytoskeleton reorganization and MAPK signaling pathway (as we already demonstrated in DLD1 cells) as well as Wnt signaling pathway and cell cycle.

Wnt Pathway Is Overexpressed in Colorectal Cancer Cells Cultured in CAF-LM CM

We showed that Wnt target genes like *E-cadherin* (Figure 1*A*) and *Snail* (Figure 1*C*; http://www.stanford.edu/group/nusselab/cgi-bin/wnt/target_genes) were overexpressed at the mRNA level. In addition, we observed that a classic Wnt target gene like *c-Myc* was overexpressed, at the protein level, in cells cultured with CM from CAF-LM (Figure 7*A*), even in APC mutant cell line (DLD1) or in an APC wild-type cell line (HCT-116).

Then, we also checked the nuclear translocation of the active form of β-catenin. As shown in Figure 7*B*, CM from CAF-LM induces nuclear translocation of β-catenin, whereas in DMEM/F12–treated cells (control), β-catenin remains localized at the cell junctions.

Discussion

The ability of mesenchymal stem cells to inhibit the proliferation of cancer cells through a cell cycle arrest at the G_1-to-S transition has recently earned much attention [13–15]. On the contrary, CAFs have always been considered to have a remarkable stimulatory effect on the proliferation of malignant epithelial cells through a paracrine mechanism [16]. Some authors reported only slight differences between the effect of breast CAFs and normal mammary fibroblasts [17] and even an inhibitory effect of normal fibroblasts compared with CAF [18]. In this study, we demonstrate that CAF-LM induce a stimulation of aggressiveness (regarding migration and invasion features of colorectal cancer cells) along with a decrease in both apoptosis and proliferation in a number of cell lines. Sustained stimulation with soluble factors secreted by hepatic CAFs induces a nonapoptotic death of colorectal cancer cells. Death-resistant cells acquired certain stemness capacity.

Here, we describe a differential proliferative response of colorectal cell lines cultured in CM from fibroblasts obtained from different locations (normal colonic mucosa, PT, and LM). NCF CM has no effect on proliferation compared with control. As expected, CAF-PT CM enhanced proliferation, but although cells depicted an arrest of cell cycle in G_1/S, the reduction of apoptosis yielded a positive balance between viability and cell death, which favors proliferation. However, interestingly, although CM of CAFs from LM clearly protected from apoptosis, the observed decrease in viability suggests a

Figure 4. (A) WST-1 proliferation assay: proliferation was measured in DLD1 (left panel) and SW480 (right panel) cells after 120 hours in culture with different CM from matched NCF and CAFs. Box plot indicates median of two experiments, eight replicates each. (B) WST-1 proliferation/viability assay: proliferation was measured in four *KRAS* mutated colorectal cell lines representing all the stages of the disease: SW1116, SW480, SW620, and DLD1 cultured with CM from nonmatched CAF-PT ($n = 6$) and CAF-LM ($n = 4$) after 8 or 12 days. Box plot indicates median of three experiments, six replicates each. After 8 days in culture, CAF-PT CM conferred more proliferative advantages than CAF-LM CM in all cell lines tested (Mann-Whitney *U* test, $P < .05$). After 12 days in culture, all cells tested (except SW480) proliferate more in CAF-PT CM than in CAF-LM CM (Mann-Whitney *U* test, $P < .05$). (C) FBS-free CM were obtained from different fibroblasts obtained from the same patient. Then, CM were supplemented with 10% FBS and used to culture DLD1 cells. Crystal violet staining of DLD1 cells after 4, 5, and 6 days of culture. Same results are obtained for all cell lines. (D) Proliferation/viability assay in *KRAS* wild-type colorectal cell lines, HT-29 (*BRAF* mutated), and Caco-2 (*KRAS* and *BRAF* wild-type) after 5 days in culture in DMEM/F12 or CM-CAF-LM. Box plot indicates median of two experiments, 12 replicates each. Relative values according to control (DMEM/F12). (E) We cultured DLD1 cells in CAF-LM CM or DMEM/F12 for 5 days, and then we seeded 10^4 cells in 96-well plates. Cells that were previously cultured with CAF-LM CM were exposed to DMEM/F12 or CAF-LM CM again. After 48 hours, cells recovered their proliferative capacity, but decreased with time. Box plot indicates median of two experiments, 12 replicates each. Relative values according to control (DMEM/F12). (F) As previously mentioned, we cultured DLD1 and HT-29 cells in CAF-LM CM or DMEM/F12 for 72 hours, and then we replated the cells at different densities in 24-well plates. As in Figure 3*F*, when we changed the culture medium from CAF-LM CM to DMEM/F12 and cells were seeded at low densities, both DLD1 and HT-29 cells seemed to lose their stem capabilities. Nevertheless, when cells were seeded at higher densities, cells restored almost all their proliferative capabilities. Inversely, when cells were cultured again with CAF-LM CM, cells acquired more stemness capacity but lost their proliferative potential.

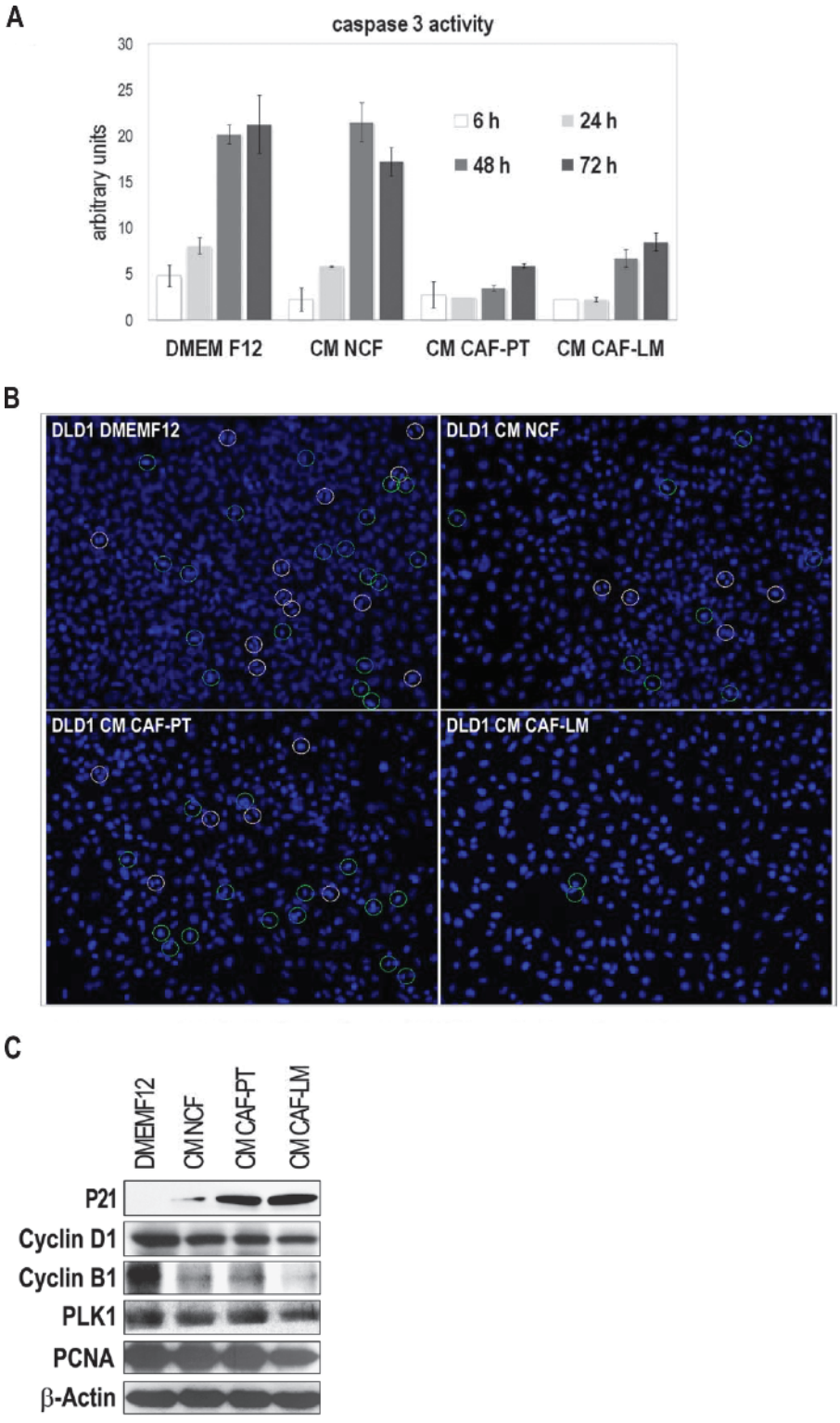

Figure 5. (A) Caspase 3 activity in DLD1 cells after 6, 24, 48, and 72 hours in culture corresponding to the adherent fraction of cells plus fraction of floating cells. Bars clearly show a protective effect of apoptosis-induced cell death in cells cultured in CAFs CM. Bars are mean values of two experiments, eight replicates each. (B) DAPI staining of DLD1 cells cultured in different CM. We synchronized and stimulated the cells with DMEM/F12 or CM from NCF, CAF-PT, or CAF-LM. After 5 days in culture, we fixed and stained the cells with DAPI. Green circumferences depict metaphases; and white circumferences, anaphases. Moreover, the intensity of DAPI staining was correlated with DNA content. Photograph displays almost all cells cultured with CAF-LM CM double DNA content (4n) without reaching cell division. (C) Mechanism of cell cycle arrest. DLD1 cells were cultured with or without different CM for 96 hours. We checked different proteins involved in cell cycle control (P21, cyclin D1 early G_1, proliferating cell nuclear antigen S-phase, cyclin B1 G_2/M transition, PLK1 M-phase). Results are representative of two different experiments.

Table 1. Percentage of Cells in Each Cell Cycle Stage Assessed by Flow Cytometric PI Staining and Analyzed with Kaluza Software.

		48 h		96 h	
		Mean	SD	Mean	SD
DMEM/F12	G_0/G_1	76.25	0.35	78.59	0.89
	S	2.63	0.52	5.60	0.83
	G_2/M	21.08	0.11	16.05	0.04
NCF CM	G_0/G_1	83.92	1.84	81.91	0.98
	S	2.86	0.78	3.43	0.66
	G_2/M	12.99	2.77	14.07	0.23
CAF-PT CM	G_0/G_1	87.53	1.60	77.08	1.63
	S	2.93	0.94	5.75	1.22
	G_2/M	9.50	0.75	16.48	0.37
CAF-LM CM	G_0/G_1	67.05	0.11	77.63	0.49
	S	2.21	0.55	1.23	0.07
	G_2/M	30.86	1.04	20.60	0.48

nonapoptotic cell death. The fact that CAFs from LM diminish the viability of cancer cells comprises a novel observation. A similar result has been described previously for mesenchymal stem cells [19,20], which is very plausible because both cell types share many similarities, especially in relation to the proteins they secrete [21]. This effect has also been recently described for adult stromal cells derived from adipose tissue in the context of pancreatic cancer [22]. However, a concomitant remarkable finding in our experiments is the generation of a highly aggressive subpopulation of CAF-LM CM–resistant tumoral cells. According to this issue, only few cells remain viable, but they seem to be reminiscent, correlating to the radiologic appearance of colorectal liver metastasis, with a central necrosis core but highly aggressive cells in the margins.

Interestingly, cells that remained attached to the plate and overcame the stimulus during CAF-LM CM exposure displayed higher

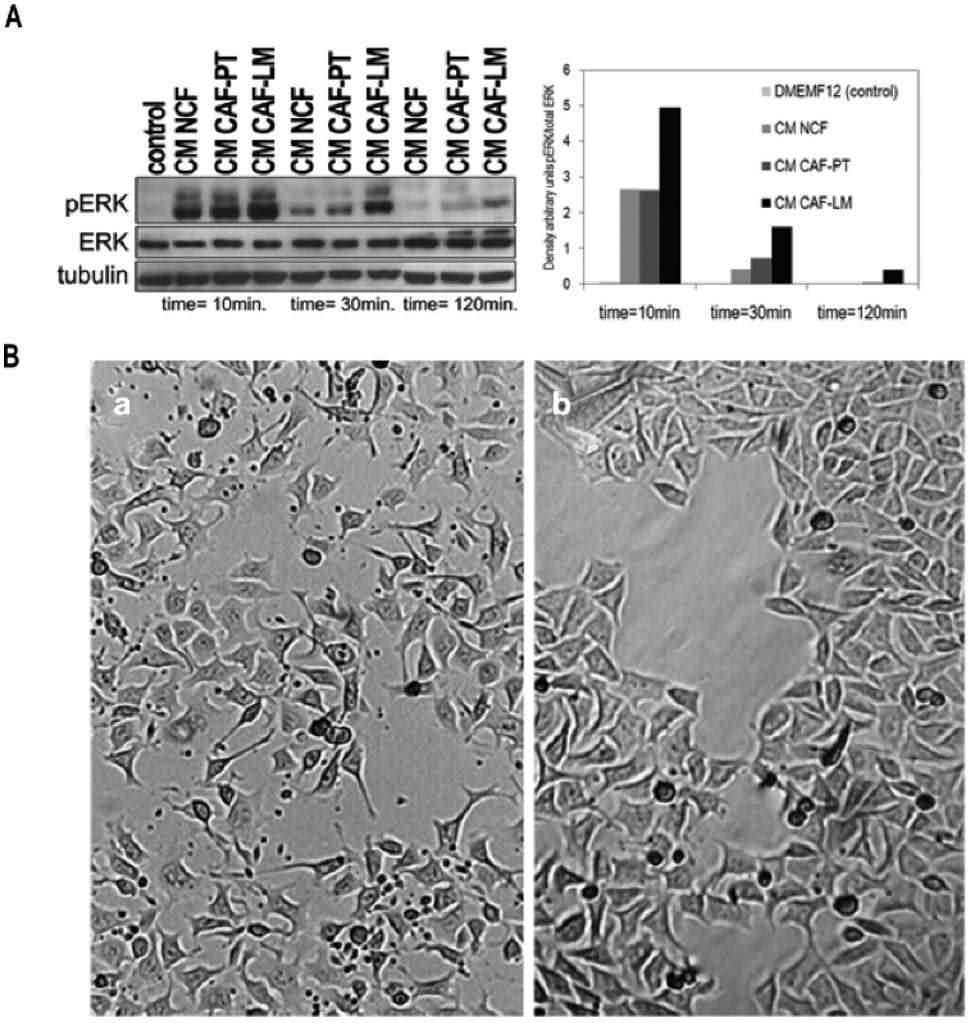

Figure 6. (A) Protein lysates from DLD1 cells treated with different CM (obtained without FBS) from NCF or CAFs (three different plates for each condition). Lysates were analyzed for ERK1/2 activation by Western blot analysis at various time points. Control cells were treated with serum-free medium alone. Levels of ERK phosphorylation were increased after 10 minutes of stimulation with all of the CM and were especially high after treatment with CAF-LM CM. After 30 minutes of stimulation, this increase was still sustained for CM from CAF-LM, whereas for the rest of CM, a decrease in phosphorylation was observed. After 120 minutes of stimulation, phosphorylation was only evident in DLD1 cells cultured in CAF-LM CM. Western blot for total ERK protein levels revealed that they were not affected by CM treatment. Graphical representation of pERK2 stimulation normalized for total ERK (evaluation using Gel Doc Quantity One software, Hercules, CA). (B) Microphotographs of DLD1 cells treated for 96 hours with CM-CAF-LM (a) or CAF-LM CM plus 20 μM MEK inhibitor U0126 (b) showing the inhibition of the cytonemes and microvesicle formation.

Table 2. Transcriptomic Data.

Probe	Gene Name	Gene Symbol	Fold Change
Overexpressed			
205869_at	Protease, serine, 1 (trypsin 1)	*PRSS1*	3.108
208719_s_at	DEAD (Asp-Glu-Ala-Asp) box polypeptide 17	*DDX17*	3.047
205321_at	Eukaryotic translation initiation factor 2, subunit 3 gamma, 52 kDa	*EIF2S3*	2.921
1554411_at	Catenin (cadherin-associated protein), beta 1, 88 kDa	*CTNNB1*	2.717
205966_at	TAF13 RNA polymerase II, TATA box binding protein (TBP)–associated factor, 18 kDa	*TAF13*	2.607
1557918_s_at	Solute carrier family 16, member 1 (monocarboxylic acid transporter 1)	*SLC16A1*	2.511
201123_s_at	Eukaryotic translation initiation factor 5A	*EIF5A*	2.507
221638_s_at	Syntaxin 16	*STX16*	2.493
220250_at	Zinc finger protein 286A	*ZNF286A*	2.484
213470_s_at	Heterogeneous nuclear ribonucleoprotein H1 (H)	*HNRNPH1*	2.459
240951_at	Hypothetical LOC283666	*LOC283666*	2.386
203311_s_at	ADP-ribosylation factor 6	*ARF6*	2.368
1558015_s_at	ARP2 actin–related protein 2 homolog (yeast)	*ACTR2*	2.355
213998_s_at	DEAD (Asp-Glu-Ala-Asp) box polypeptide 17	*DDX17*	2.25
214786_at	Mitogen-activated protein kinase kinase kinase 1	*MAP3K1*	2.218
223940_x_at	Metastasis-associated lung adenocarcinoma transcript 1 (non–protein coding)	*MALAT1*	2.175
1553962_s_at	*ras* homolog gene family, member B	*RHOB*	2.17
224568_x_at	Metastasis-associated lung adenocarcinoma transcript 1 (non–protein coding)	*MALAT1*	2.16
208151_x_at	DEAD (Asp-Glu-Ala-Asp) box polypeptide 17	*DDX17*	2.142
1553219_a_at	Alport syndrome, mental retardation, midface hypoplasia and elliptocytosis chromosomal region, gene 1	*AMMECR1*	2.129
201130_s_at	Cadherin 1, type 1, E-cadherin (epithelial)	*CDH1*	2.128
210734_x_at	MYC-associated factor X	*MAX*	2.127
205822_s_at	3-Hydroxy-3-methylglutaryl-coenzyme A synthase 1 (soluble)	*HMGCS1*	2.115
235563_at	CDNA clone IMAGE: 6025865	—	2.114
230397_at	Transcribed locus	—	2.075
205402_x_at	Protease, serine, 2 (trypsin 2)	*PRSS2*	2.057
243054_at	Transcribed locus	—	2.046
206184_at	v-*crk* sarcoma virus CT10 oncogene homolog (avian)-like	*CRKL*	2.039
200641_s_at	Tyrosine 3-monooxygenase/tryptophan 5-monooxygenase activation protein, zeta polypeptide	*YWHAZ*	2.033
244030_at	Serine/threonine/tyrosine interacting protein /// similar to serine/threonine/tyrosine interacting protein	*STYX*	2.009
243490_at	—	—	2.009
218340_s_at	Ubiquitin-like modifier activating enzyme 6	*UBA6*	2.006
201856_s_at	Zinc finger RNA binding protein	*ZFR*	2.002
Downregulated			
237241_at	Epithelial cell–transforming sequence 2 oncogene	*ECT2*	0.084
1554436_a_at	Regenerating islet-derived family, member 4	*REG4*	0.093
223447_at	Regenerating islet-derived family, member 4	*REG4*	0.118
238984_at	Regenerating islet-derived family, member 4	*REG4*	0.132
220651_s_at	Minichromosome maintenance complex component 10	*MCM10*	0.133
201890_at	Ribonucleotide reductase M2 polypeptide	*RRM2*	0.137
229551_x_at	Zinc finger protein 367	*ZNF367*	0.152
221521_s_at	GINS complex subunit 2 (Psf2 homolog)	*GINS2*	0.155
212020_s_at	Antigen identified by monoclonal antibody Ki-67	*MKI67*	0.16
219306_at	Kinesin family member 15	*KIF15*	0.16
229305_at	MLF1 interacting protein	*MLF1IP*	0.168
219918_s_at	Asp (abnormal spindle) homolog, microcephaly associated (*Drosophila*)	*ASPM*	0.17
205034_at	Cyclin E2	*CCNE2*	0.178
204318_s_at	G_2 and S-phase expressed 1	*GTSE1*	0.18
222962_s_at	Minichromosome maintenance complex component 10	*MCM10*	0.182
202534_x_at	Dihydrofolate reductase	*DHFR*	0.186
235609_at	Transcribed locus	—	0.188
236641_at	Kinesin family member 14	*KIF14*	0.197
206633_at	Cholinergic receptor, nicotinic, alpha 1 (muscle)	*CHRNA1*	0.197
204026_s_at	ZW10 interactor	*ZWINT*	0.198
209891_at	SPC25, NDC80 kinetochore complex component, homolog (*Saccharomyces cerevisiae*)	*SPC25*	0.198
218585_s_at	Denticleless homolog (*Drosophila*)	*DTL*	0.2
204126_s_at	CDC45 cell division cycle 45-like (*S. cerevisiae*)	*CDC45L*	0.203
48808_at	Dihydrofolate reductase	*DHFR*	0.203
207746_at	Polymerase (DNA directed), theta	*POLQ*	0.204
218883_s_at	MLF1 interacting protein	*MLF1IP*	0.208
204531_s_at	Breast cancer 1, early onset	*BRCA1*	0.212
222680_s_at	Denticleless homolog (*Drosophila*)	*DTL*	0.213
202240_at	Polo-like kinase 1 (*Drosophila*)	*PLK1*	0.218
204603_at	Exonuclease 1	*EXO1*	0.218

Table 2. (*continued*)

Probe	Gene Name	Gene Symbol	Fold Change
219493_at	SHC SH2-domain binding protein 1	*SHCBP1*	0.218
219502_at	nei endonuclease VIII-like 3 (*Escherichia coli*)	*NEIL3*	0.22
213007_at	Fanconi anemia, complementation group I	*FANCI*	0.222
211814_s_at	Cyclin E2	*CCNE2*	0.226
212949_at	Non-SMC condensin I complex, subunit H	*NCAPH*	0.229
1565823_at	Transcribed locus	—	0.229
213747_at	Similar to hCG15011	*LOC100134128*	0.231
209773_s_at	Ribonucleotide reductase M2 polypeptide	*RRM2*	0.231
215942_s_at	G_2 and S-phase expressed 1	*GTSE1*	0.233
204146_at	RAD51-associated protein 1	*RAD51AP1*	0.233
201292_at	Topoisomerase (DNA) II alpha 170 kDa	*TOP2A*	0.233
204128_s_at	Replication factor C (activator 1) 3, 38 kDa	*RFC3*	0.234
202589_at	Thymidylate synthetase	*TYMS*	0.235
212023_s_at	Antigen identified by monoclonal antibody Ki-67	*MKI67*	0.237
205046_at	Centromere protein E, 312 kDa	*CENPE*	0.239
202532_s_at	Dihydrofolate reductase	*DHFR*	0.241
223307_at	Cell division cycle–associated 3	*CDCA3*	0.241
235545_at	DEP domain containing 1	*DEPDC1*	0.242
226456_at	Chromosome 16 open reading frame 75	*C16orf75*	0.245
204962_s_at	Centromere protein A	*CENPA*	0.245
202095_s_at	Baculoviral IAP repeat-containing 5 (survivin)	*BIRC5*	0.246
218663_at	Non-SMC condensin I complex, subunit G	*NCAPG*	0.248
209709_s_at	Hyaluronan-mediated motility receptor (RHAMM)	*HMMR*	0.249

Specific deregulated genes in DLD1 cells cultured in CM from hepatic CAFs.

clonogenic potential, which suggests that CAFs from LM have the ability to stimulate the development of a stem cell niche. Actually, it has been described that cells surrounding the cancer stem cells not only maintain a high Wnt activity but also are able to induce Wnt signaling pathway in more differentiated cells and may further restore clonogenicity [23]. In addition, those cells cultured in CM from CAF-LM seem to recapitulate the features of an EMT more efficiently than cells exposed to other CM (from PT or NCF). This fact may explain the decrease in proliferation because it is known that, when cells move and migrate, they slow down their cell cycle because they dedicate all their machinery to migrate and not to proliferate, in a process controlled by Snail [24]. Interestingly, in our model, cells cultured in NCF CM and CAF-PT CM arrest their cell cycle at G1/S, but when cultured in CAF-LM CM, the cell cycle was stopped at G_2/M. The levels of P21 in cells cultured in CAF-PT CM confirm the regular G_1/S control because P21 is an inhibitor of cdk2 and cdk4. However, P21 induction was found also to inhibit the expression of multiple proteins involved in the execution and control of mitosis [25,26]. Moreover, it has been reported that P21-induced depletion of the cellular pools of mitosis control proteins was followed by asynchronous resynthesis of such proteins after their release from P21 [27], which may explain the observed mitotic abnormalities.

Table 3. Gene Ontology.

Category	Term	Count	*P*	Fold Enrichment	FDR
Gene ontology, overexpressed					
GOTERM_BP_ALL	GO:0009611~response to wounding	48	8.437*e* – 09	2.503	1.494*e* – 05
GOTERM_BP_ALL	GO:0050896~response to stimulus	156	1.628*e* – 07	1.441	2.882*e* – 04
GOTERM_BP_ALL	GO:0009605~response to external stimulus	62	1.092*e* – 06	1.899	1.933*e* – 03
GOTERM_BP_ALL	GO:0048518~positive regulation of biologic process	112	1.950*e* – 06	1.522	3.453*e* – 03
GOTERM_BP_ALL	GO:0002376~immune system process	63	3.176*e* – 06	1.827	5.623*e* – 03
GOTERM_BP_ALL	GO:0042221~response to chemical stimulus	79	5.164*e* – 06	1.660	9.144*e* – 03
GOTERM_BP_ALL	GO:0006955~immune response	47	5.767*e* – 06	2.024	1.021*e* – 02
GOTERM_BP_ALL	GO:0006950~response to stress	92	1.370*e* – 05	1.543	2.425*e* – 02
GOTERM_BP_ALL	GO:0042060~wound healing	21	1.695*e* – 05	3.045	3.001*e* – 02
GOTERM_BP_ALL	GO:0009607~response to biotic stimulus	30	2.799*e* – 05	2.356	4.954*e* – 02
Gene ontology, downregulated					
GOTERM_BP_ALL	GO:0007049~cell cycle	55	1.772*e* – 41	9.396	2.767*e* – 38
GOTERM_BP_ALL	GO:0000279~M phase	39	1.041*e* – 36	16.199	1.626*e* – 33
GOTERM_BP_ALL	GO:0022403~cell cycle phase	42	2.277*e* – 36	13.370	3.555*e* – 33
GOTERM_BP_ALL	GO:0022402~cell cycle process	45	1.426*e* – 34	10.431	2.226*e* – 31
GOTERM_BP_ALL	GO:0007067~mitosis	32	5.066*e* – 32	19.326	7.908*e* – 29
GOTERM_BP_ALL	GO:0000280~nuclear division	32	5.066*e* – 32	19.326	7.908*e* – 29
GOTERM_BP_ALL	GO:0000087~M phase of mitotic cell cycle	32	1.019*e* – 31	18.917	1.591*e* – 28
GOTERM_BP_ALL	GO:0048285~organelle fission	32	2.016*e* – 31	18.525	3.148*e* – 28
GOTERM_BP_ALL	GO:0000278~mitotic cell cycle	37	1.779*e* – 30	12.490	2.778*e* – 27
GOTERM_BP_ALL	GO:0006260~DNA replication	28	1.177*e* – 27	19.193	1.838*e* – 24

Table 4. GSEA Summary.

KEGG Pathway Name	Size	ES	NES	NOM *P*	FDR *q*	FWER *P*
HSA04520_ADHERENS_JUNCTION	74	0.319	2.900	0.000*e* + 00	0.000	0.001
HSA05130_PATHOGENIC_ESCHERICHIA_COLI_INFECTION_EHEC	47	0.399	2.948	0.000*e* + 00	0.001	0.001
HSA05131_PATHOGENIC_ESCHERICHIA_COLI_INFECTION_EPEC	47	0.399	2.973	0.000*e* + 00	0.001	0.001
HSA05212_PANCREATIC_CANCER	73	0.317	2.812	0.000*e* + 00	0.001	0.002
HSA04010_MAPK_SIGNALING_PATHWAY	247	0.183	2.665	0.000*e* + 00	0.001	0.003
HSA05220_CHRONIC_MYELOID_LEUKEMIA	75	0.268	2.426	2.972*e* − 03	0.003	0.019
HSA05210_COLORECTAL_CANCER	84	0.243	2.331	0.000*e* + 00	0.007	0.046
HSA05110_CHOLERA_INFECTION	41	0.318	2.257	0.000*e* + 00	0.010	0.077
HSA05213_ENDOMETRIAL_CANCER	52	0.285	2.229	0.000*e* + 00	0.011	0.091
HSA04510_FOCAL_ADHESION	189	0.167	2.219	1.410*e* − 03	0.011	0.098
HSA04662_B_CELL_RECEPTOR_SIGNALING_PATHWAY	61	0.266	2.213	1.541*e* − 03	0.010	0.103
HSA05215_PROSTATE_CANCER	86	0.235	2.199	0.000*e* + 00	0.010	0.112
HSA04514_CELL_ADHESION_MOLECULES	129	0.194	2.189	1.391*e* − 03	0.009	0.117
HSA04310_WNT_SIGNALING_PATHWAY	143	0.187	2.192	0.000*e* + 00	0.010	0.117
HSA04810_REGULATION_OF_ACTIN_CYTOSKELETON	196	0.165	2.174	0.000*e* + 00	0.010	0.136
HSA04110_CELL_CYCLE	109	0.198	2.130	1.441*e* − 03	0.012	0.172

ES indicates enrichment score; NES, normalized enrichment score; NOM *P*, nominal *P* value.

Thus, the high level of P21 observed by immunoblot correlates with the transcriptomic data in relation to the inhibition of several genes that regulate G_2/M control and mitosis.

Therefore, the transcriptomic profile, experimental data, gene ontology, and GSEA are consistent with this G_2/M arrest.

Another remarkable finding is that cells cultured in CAF-LM CM, which are resistant to apoptosis, can be induced to die by nonapoptotic mechanisms such as necrosis, which has been evidenced by the large quantity of floating cells in our *in vitro* model. It is well known that most tumor cells and, in particular, those of solid tumors maintain the uniqueness of remaining dormant or suffering nonapoptotic cell death. In addition, the proportion of tumor cells that undergo nonapoptotic cell death increases if apoptosis is inhibited [28]. This might explain how the stromal microenvironment induces both insensitivity to apoptosis and increased clonogenic potential on epithelial cells. Moreover, after 48 hours of culture in CAF-LM CM, DLD1 cells acquired particular morphologic changes that correspond to cytonemes and tunneling nanotubule formation. This phenotype resembles a neuronal cell type, which is reverted with anti-ERK agents. The morphologic changes are probably the consequence of down-regulation of tight cell-cell contacts, a necessary event for migration and motility [29]. Thus, such phenotypic alterations, both proliferative and morphologic, have to be understood as multifactorial processes and are not attributable to only one factor. However, it is clear that such a transformation

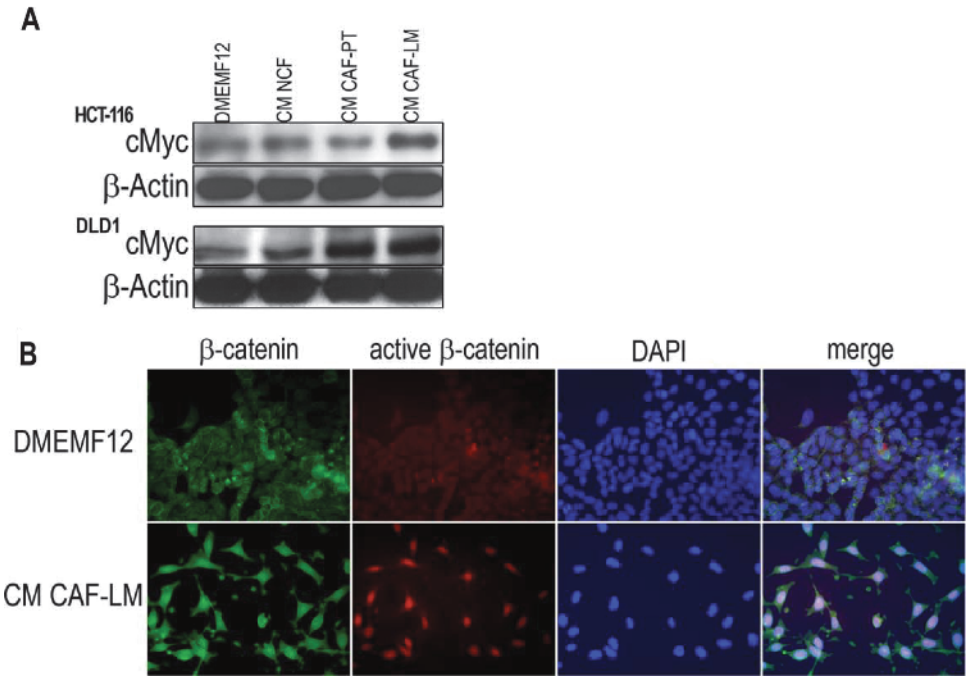

Figure 7. (A) We checked the overexpression of one of the classic targets of Wnt pathway in colorectal cancer, cMyc. We used an APC wild-type cell line (HCT-116) and a mutated APC cell line (DLD1). In both cells lines, overexpression of cMyc was evident, but it was clearer on the APC wild-type, where the Wnt pathway is not constitutively activated. Results are representative of two different experiments. (B) Translocation of β-catenin to the cell nucleus, one of the final events of Wnt pathway. After 72 hours in culture, we observed not only the overexpression of β-catenin but also the translocation of the active form to the DLD1 nucleus.

(in the context of change in shape) depends on soluble factors released by CAF-LM, which induce a particular transcriptional program in the epithelial cells. Accordingly, *CTNNB1*, *ARF6*, *ACTR2*, and *RHOB* are involved in cytoskeleton remodeling. It is also known that β-catenin (*CTNNB1*) overexpression inhibits proliferation and enhances neurite formation in neuroblastoma cell lines [30]. In addition, we also observed a down-regulation of *MKI67*. These genes could, at least in part, contribute to the low proliferative levels observed. Moreover, *ARF6* regulates tumorigenic and invasive cellular properties, and cells overexpressing *ARF6* display the phenotype we observed [31]. Another overrepresented gene is *DDX17*, an RNA helicase involved in neuronal differentiation and directly involved in colorectal cancer prognosis [32,33].

We also observed overexpression of *MAP3K1*, which is an important regulator of Ras/ERK pathway and is also involved in the canonical Wnt signaling pathway; it positively regulates expression of Wnt target genes [34], as depicted by the GSEA. The activation of these two signaling pathways has been experimentally demonstrated in our cells stimulated with CM from CAF-LM. Signal duration of ERK activation regulates cell fate [35]. Sustained, but not transient, activation of ERK signaling preceded the differentiation of PC12 pheochromocytoma cells into sympathetic-like neurons [36]. This cell behavior has also been reported in fibroblasts [37]. Therefore, the differential composition of factors secreted by hepatic CAFs could explain the sustained activation of ERK that we describe. The addition of MEK and ERK inhibitors to CAF-LM CM–stimulated DLD1 cells inhibited the formation of cytonemes, probably because the inhibition of motility processes kept cells in a tethered conformation. As expected, ERK inhibitor U0126 did not restore the proliferation levels in CAF-LM CM–cultured colorectal cancer cells.

In conclusion, the ability of malignant cells to settle and grow at a distance depends on the microenvironment, apart from their genetic background. Moreover, it is often said that metastatic cells have acquired different genetic alterations that confer them to be potentially more aggressive. However, most tumor cells are poorly adapted to survive in an environment that is not their own. Here, we demonstrate that, based on the same genetic background (without adding any genetic alteration represented by each of the colorectal cell lines), liver microenvironment induces an impairment of proliferation alongside the promotion of migrating and invading capabilities of colorectal cells, which further become more aggressive. This suggests that those cells that survive and adapt may succeed and develop an adaptive phenotype, in a darwinian sense, and depending on the stimuli of the surrounding stroma. Besides this, some products secreted by CAF-LM may act as a trigger to develop stemness capacity in cancer cell populations (probably at the tumor edges regarding the morphology of a liver metastasis) and promote the spread and increased aggressiveness of cancer cells. It has been recently described that Snail and Twist are able to generate cancer stem cells from more differentiated tumor cells [38]. The reversibility of the phenotype when removing the stimulus suggests that there is no selected trait. Simultaneously, CAFs from LM induce nonapoptotic cancer cell death as a consequence of induction of insensitivity to apoptosis. This cell death is probably related with the P21 cell cycle arrest. Cells that overcome such stimuli and are able to reenter the cell cycle after such a high-level induction of P21 may contribute to carcinogenesis and tumor progression.

Future lines of research should be focused on identifying the biologic mechanisms underlying both cell death and stemness capacity, under the influence of liver metastasis microenvironment, to find new strategies for the treatment of metastatic colorectal cancer.

References

[1] Schauer IG, Sood AK, Mok S, and Liu J (2011). Cancer-associated fibroblasts and their putative role in potentiating the initiation and development of epithelial ovarian cancer. *Neoplasia* **13**, 393–405.

[2] Joyce JA and Pollard JW (2009). Microenvironmental regulation of metastasis. *Nat Rev* **9**, 239–252.

[3] Kalluri R and Zeisberg M (2006). Fibroblasts in cancer. *Nat Rev* **6**, 392–401.

[4] Alphonso A and Alahari SK (2009). Stromal cells and integrins: conforming to the needs of the tumor microenvironment. *Neoplasia* **11**, 1264–1271.

[5] Orimo A, Gupta PB, Sgroi DC, Arenzana-Seisdedos F, Delaunay T, Naeem R, Carey VJ, Richardson AL, and Weinberg RA (2005). Stromal fibroblasts present in invasive human breast carcinomas promote tumor growth and angiogenesis through elevated SDF-1/CXCL12 secretion. *Cell* **121**, 335–348.

[6] Gout S and Huot J (2008). Role of cancer microenvironment in metastasis: focus on colon cancer. *Cancer Microenviron* **1**, 69–83.

[7] Fabra A, Nakajima M, Bucana CD, and Fidler IJ (1992). Modulation of the invasive phenotype of human colon carcinoma cells by organ specific fibroblasts of nude mice. *Differentiation* **52**, 101–110.

[8] Morin PJ (2003). Drug resistance and the microenvironment: nature and nurture. *Drug Resist Updat* **6**, 169–172.

[9] Linn SC, West RB, Pollack JR, Zhu S, Hernandez-Boussard T, Nielsen TO, Rubin BP, Patel R, Goldblum JR, Siegmund D, et al. (2003). Gene expression patterns and gene copy number changes in dermatofibrosarcoma protuberans. *Am J Pathol* **163**, 2383–2395.

[10] Irizarry RA, Hobbs B, Collin F, Beazer-Barclay YD, Antonellis KJ, Scherf U, and Speed TP (2003). Exploration, normalization, and summaries of high density oligonucleotide array probe level data. *Biostatistics* **4**, 249–264.

[11] Tibshirani R (2006). A simple method for assessing sample sizes in microarray experiments. *BMC Bioinformatics* **7**, 106.

[12] Subramanian A, Kuehn H, Gould J, Tamayo P, and Mesirov JP (2007). GSEA-P: a desktop application for Gene Set Enrichment Analysis. *Bioinformatics* **23**, 3251–3253.

[13] Sun B, Yu KR, Bhandari DR, Jung JW, Kang SK, and Kang KS (2010). Human umbilical cord blood mesenchymal stem cell–derived extracellular matrix prohibits metastatic cancer cell MDA-MB-231 proliferation. *Cancer Lett* **296**, 178–185.

[14] Li L, Tian H, Chen Z, Yue W, Li S, and Li W (2011). Inhibition of lung cancer cell proliferation mediated by human mesenchymal stem cells. *Acta Biochim Biophys Sin (Shanghai)* **43**, 143–148.

[15] Zhu Y, Sun Z, Han Q, Liao L, Wang J, Bian C, Li J, Yan X, Liu Y, Shao C, et al. (2009). Human mesenchymal stem cells inhibit cancer cell proliferation by secreting DKK-1. *Leukemia* **23**, 925–933.

[16] Wels J, Kaplan RN, Rafii S, and Lyden D (2008). Migratory neighbors and distant invaders: tumor-associated niche cells. *Genes Dev* **22**, 559–574.

[17] Lebret SC, Newgreen DF, Thompson EW, and Ackland ML (2007). Induction of epithelial to mesenchymal transition in PMC42-LA human breast carcinoma cells by carcinoma-associated fibroblast secreted factors. *Breast Cancer Res* **9**, R19.

[18] Adams EF, Newton CJ, Tait GH, Braunsberg H, Reed MJ, and James VH (1988). Paracrine influence of human breast stromal fibroblasts on breast epithelial cells: secretion of a polypeptide which stimulates reductive 17β-oestradiol dehydrogenase activity. *Int J Cancer* **42**, 119–122.

[19] Ramasamy R, Lam EW, Soeiro I, Tisato V, Bonnet D, and Dazzi F (2007). Mesenchymal stem cells inhibit proliferation and apoptosis of tumor cells: impact on *in vivo* tumor growth. *Leukemia* **21**, 304–310.

[20] Qiao L, Xu Z, Zhao T, Zhao Z, Shi M, Zhao RC, Ye L, and Zhang X (2008). Suppression of tumorigenesis by human mesenchymal stem cells in a hepatoma model. *Cell Res* **18**, 500–507.

[21] Klopp AH, Gupta A, Spaeth E, Andreeff M, and Marini F III (2011). Concise review: dissecting a discrepancy in the literature: do mesenchymal stem cells support or suppress tumor growth? *Stem Cells* **29**, 11–19.

[22] Cousin B, Ravet E, Poglio S, De Toni F, Bertuzzi M, Lulka H, Touil I, Andre M, Grolleau JL, Peron JM, et al. (2009). Adult stromal cells derived from human adipose tissue provoke pancreatic cancer cell death both *in vitro* and *in vivo*. *PLoS One* **4**, e6278.

[23] Vermeulen L, De Sousa EMF, van der Heijden M, Cameron K, de Jong JH, Borovski T, Tuynman JB, Todaro M, Merz C, Rodermond H, et al. (2010). Wnt activity defines colon cancer stem cells and is regulated by the microenvironment. *Nat Cell Biol* **12**, 468–476.

[24] Vega S, Morales AV, Ocana OH, Valdes F, Fabregat I, and Nieto MA (2004). Snail blocks the cell cycle and confers resistance to cell death. *Genes Dev* **18**, 1131–1143.

[25] Matsumoto Y, Hayashi K, and Nishida E (1999). Cyclin-dependent kinase 2 (Cdk2) is required for centrosome duplication in mammalian cells. *Curr Biol* **9**, 429–432.

[26] Chang BD, Watanabe K, Broude EV, Fang J, Poole JC, Kalinichenko TV, and Roninson IB (2000). Effects of $p21^{Waf1/Cip1/Sdi1}$ on cellular gene expression: implications for carcinogenesis, senescence, and age-related diseases. *Proc Natl Acad Sci USA* **97**, 4291–4296.

[27] Chang BD, Broude EV, Fang J, Kalinichenko TV, Abdryashitov R, Poole JC, and Roninson IB (2000). $p21^{Waf1/Cip1/Sdi1}$-induced growth arrest is associated with depletion of mitosis-control proteins and leads to abnormal mitosis and endoreduplication in recovering cells. *Oncogene* **19**, 2165–2170.

[28] Brown JM and Wouters BG (1999). Apoptosis, p53, and tumor cell sensitivity to anticancer agents. *Cancer Res* **59**, 1391–1399.

[29] Sherer NM and Mothes W (2008). Cytonemes and tunneling nanotubules in cell-cell communication and viral pathogenesis. *Trends Cell Biol* **18**, 414–420.

[30] Sangkhathat S, Nara K, Kusafuka T, Yoneda A, and Fukuzawa M (2006). Artificially accumulated β-catenin inhibits proliferation and induces neurite extension of neuroblastoma cell line NB-1 via up-regulation of trkA. *Oncol Rep* **16**, 1197–1203.

[31] Muralidharan-Chari V, Hoover H, Clancy J, Schweitzer J, Suckow MA, Schroeder V, Castellino FJ, Schorey JS, and D'Souza-Schorey C (2009). ADP-ribosylation factor 6 regulates tumorigenic and invasive properties *in vivo*. *Cancer Res* **69**, 2201–2209.

[32] Shin S, Rossow KL, Grande JP, and Janknecht R (2007). Involvement of RNA helicases p68 and p72 in colon cancer. *Cancer Res* **67**, 7572–7578.

[33] Ip FC, Chung SS, Fu WY, and Ip NY (2000). Developmental and tissue-specific expression of DEAD box protein p72. *Neuroreport* **11**, 457–462.

[34] Sue Ng S, Mahmoudi T, Li VS, Hatzis P, Boersema PJ, Mohammed S, Heck AJ, and Clevers H (2010). MAP3K1 functionally interacts with Axin1 in the canonical Wnt signalling pathway. *Biol Chem* **391**, 171–180.

[35] Murphy LO and Blenis J (2006). MAPK signal specificity: the right place at the right time. *Trends Biochem Sci* **31**, 268–275.

[36] Robbins DJ, Cheng M, Zhen E, Vanderbilt CA, Feig LA, and Cobb MH (1992). Evidence for a Ras-dependent extracellular signal–regulated protein kinase (ERK) cascade. *Proc Natl Acad Sci USA* **89**, 6924–6928.

[37] Mansour SJ, Matten WT, Hermann AS, Candia JM, Rong S, Fukasawa K, Vande Woude GF, and Ahn NG (1994). Transformation of mammalian cells by constitutively active MAP kinase kinase. *Science* **265**, 966–970.

[38] Mani SA, Guo W, Liao MJ, Eaton EN, Ayyanan A, Zhou AY, Brooks M, Reinhard F, Zhang CC, Shipitsin M, et al. (2008). The epithelial-mesenchymal transition generates cells with properties of stem cells. *Cell* **133**, 704–715.